J|A|C|S
ARTICLES
Published on Web 12/04/2002

Ultrafast Processes in Bimetallic Dyads with Extended Aromatic Bridges. Energy and Electron Transfer Pathways in Tetrapyridophenazine-Bridged Complexes

Claudio Chiorboli,[†] Michael A. J. Rodgers,[‡] and Franco Scandola*[,†,§]

Contribution from the ISOF-CNR Sezione di Ferrara, Via L. Borsari 46, 44100 Ferrara, Italy, Department of Chemistry, Bowling Green State University, Bowling Green, Ohio 43403, and Dipartimento di Chimica, Università di Ferrara, Via L. Borsari 46, 44100 Ferrara, Italy

Received September 10, 2002; E-mail: snf@unife.it

Abstract: The energy and electron transfer processes taking place in binuclear polypyridine complexes of ruthenium and osmium based on the tetrapyrido[3,2-*a*:2′,3′-*c*:3″,2″-*h*:2‴,3‴-*j*]phenazine bridging ligand (tpphz) have been investigated by ultrafast absorption spectroscopy. In the binuclear complexes, each chromophore is characterized by two spectrally distinguishable metal-to-ligand charge transfer (MLCT) excited states: $MLCT_1$ (with promoted electron mainly localized on the bpy-like portion of tpphz, higher energy) and $MLCT_0$ (with promoted electron mainly localized on the pyrazine-like portion of tpphz, lower energy). In the homodinuclear complexes Ru(II)−Ru(II) and Os(II)−Os(II), $MLCT_1 \rightarrow MLCT_0$ relaxation (intraligand electron transfer) is observed, with strongly solvent-dependent kinetics (ca. 10^{-10} s in CH_2Cl_2, ca. 10^{-12} s in CH_3CN). In the heterodinuclear Ru(II)−Os(II) complex, *Ru(II)−Os(II) → Ru(II)−*Os(II) energy transfer takes place by two different sequences of time-resolved processes, depending on the solvent: (a) in CH_2Cl_2, ruthenium-to-osmium energy transfer at the $MLCT_1$ level followed by $MLCT_1 \rightarrow MLCT_0$ relaxation in the osmium chromophore, (b) in CH_3CN, $MLCT_1 \rightarrow MLCT_0$ relaxation in the ruthenium chromophore followed by osmium-to-ruthenium metal-to-metal electron transfer. In the mixed-valence Ru(II)−Os(III) species, the *Ru(II)−Os(III) → Ru(III)−Os(II) electron transfer quenching is found to proceed by two consecutive steps in CH_3CN: intraligand electron transfer followed by ligand-to-metal electron transfer. On a longer time scale, charge recombination leads back to the ground state. Altogether, the results show that the tpphz bridge plays an active mechanistic role in these systems, efficiently mediating the transfer processes with its electronic levels.

Introduction

The study of photoinduced processes in covalently linked donor−acceptor systems ("dyads", "polyads") has been an active area of research for the last two decades,[1−4] with relevant results in terms of both fundamental knowledge (experimental verification of electron and energy transfer theories)[2] and potential applications (interesting light-induced functions,[1] such as, e.g., charge separation[3] and antenna effect[5,6]). In the inorganic domain,[4] the donor and acceptor molecular components are usually metal complexes, typically of the polypyridine family. The covalent linkages between donor and acceptor are provided by appropriate bridging ligands. The role of the bridging groups is not only structural, however, as it has been shown that their nature has profound effects on the electron and energy transfer rates.[2,4] Thus, the bridges are sometimes indicated, using an appealing (although mechanistically incorrect) similarity, as "molecular wires".[7] The detailed understanding of the active role of the bridge is a subject of considerable interest in the study of photoinduced electron and energy transfer in covalently linked systems.

Tetrapyrido[3,2-*a*:2′,3′-*c*:3″,2″-*h*:2‴,3‴-*j*]phenazine, tpphz, is an interesting fully aromatic bridging ligand. It has been recently used in the design and synthesis of a variety of dyads[8−10] and tetrads[10,11] suitable for the study of intramolecular

[†] ISOF-CNR Sezione di Ferrara.
[‡] Bowling Green State University.
[§] Università di Ferrara.

(1) Balzani, V.; Scandola, F. *Supramolecular Photochemistry*; Horwood: Chichester, U.K., 1991.
(2) Paddon-Row, M. N. In *Electron Transfer in Chemistry*; Balzani, V., Ed.; Wiley-VCH: Weinheim, 2001; Vol. III, Chapter 2.1, pp 179−271 and refs therein.
(3) Gust, D.; Moore, T. A.; Moore, A. L. In *Electron Transfer in Chemistry*; Balzani, V., Ed.; Wiley-VCH: Weinheim, 2001; Vol. III, Chapter 2.2, pp 272−336 and refs therein.
(4) Scandola, F.; Chiorboli, C.; Indelli, M. T.; Rampi, M. A. In *Electron Transfer in Chemistry*; Balzani, V., Ed.; Wiley-VCH: Weinheim, 2001; Vol. III, Chapter 2.3, pp 337−408 and refs therein.
(5) Hsiao, J.-S.; Krueger, B. P.; Wagner, R. W.; Johnson, T. E.; Delaney, J. K.; Mauzerall, D. C.; Fleming, G. R.; Lindsey, J. S.; Bocian, D. F.; Donohoe, R. J. *J. Am. Chem. Soc.* **1996**, *118*, 11181−11193.
(6) Campagna, S.; Serroni, S.; Puntoriero, F.; Di Pietro, C.; Ricevuto, V. In *Electron Transfer in Chemistry*; Balzani, V., Ed.; Wiley-VCH: Weinheim, 2001; Vol. V, Chapter 1.6, pp 186−214 and refs therein.
(7) De Cola, L.; Belser, P. In *Electron Transfer in Chemistry*; Balzani, V., Ed.; Wiley-VCH: Weinheim, 2001; Vol. V, Chapter 1.3, pp 97−136 and refs therein.
(8) Bolger, J.; Gourdon, A.; Ishow, E.; Launay, J. P. *Inorg. Chem.* **1996**, *35*, 2937−2944.
(9) Chiorboli, C.; Bignozzi, C. A.; Scandola, F.; Ishow, E.; Gourdon, A.; Launay, J. P. *Inorg. Chem.* **1999**, *38*, 2402−2410.
(10) Campagna, S.; Serroni, S.; Bodige, S.; MacDonnell, F. M. *Inorg. Chem.* **1999**, *38*, 692−701.

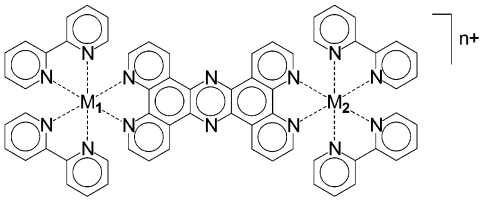

Ru(II)-Ru(II)	$M_1 = M_2 = Ru$, n = 4
Os(II)-Os(II)	$M_1 = M_2 = Os$, n = 4
Ru(II)-Os(II)	$M_1 = Ru$, $M_2 = Os$, n = 4
Ru(II)-Os(III)	$M_1 = Ru$, $M_2 = Os$, n = 5

photoinduced energy or electron transfer. Related more extended aromatic bridging ligands have also been recently developed.[12,13]

In previous studies, the homodinuclear complexes $[(bpy)_2Ru(tpphz)Ru(bpy)_2]^{4+}$, **Ru(II)−Ru(II)**, and $[(bpy)_2Os(tpphz)Os(bpy)_2]^{4+}$, **Os(II)−Os(II)**, were investigated by spectroscopic, electrochemical, and standard photophysical techniques.[8,9,10] The main conclusions from previous work can be summarized as follows: (a) in the ground state, the binuclear complexes can be described as supramolecular systems with relatively weak intercomponent interaction; (b) in all of the binuclear species, the lowest emitting metal-to-ligand charge transfer (MLCT) excited states involve the tpphz bridge; (c) two types of MLCT states involving the bridging ligand are present in these complexes (as schematically shown in Figure 1): $MLCT_1$, mainly involving the bipyridine-like moiety of the bridge (substantial electron density on coordinated nitrogens), and $MLCT_0$, mainly involving the pyrazine-like moiety of the bridge (substantial electron density on central nitrogens);[14,15](d) states of type $MLCT_1$ are involved in absorption; (e) at room temperature, emission takes place from states of the $MLCT_0$ type; and (f) the $MLCT_0$ states are substantially stabilized in polar solvents, leading to pronounced red shift and lifetime shortening of the emission.

Recently, Flamigni et al.[16] succeeded in observing by picosecond absorption and emission spectroscopy the $MLCT_1 \rightarrow MLCT_0$ conversion in the Ru−Ru homodinuclear complex in CH_2Cl_2.

The heterodinuclear complex $[(bpy)_2Ru(tpphz)Os(bpy)_2]^{4+}$, **Ru(II)−Os(II)**, was also studied.[9] Consistent with the behavior of other Ru(II)−Os(II) polypyridine complexes, the conventional photophysics indicated that 100% efficient and rapid (<10 ns) Ru(II)-to-Os(II) energy transfer takes place in this system. At room temperature, the emission takes place, regardless of excitation wavelength, from the lowest Os-based $MLCT_0$ excited state.

The photophysics of $[(bpy)_2Ru(tpphz)Os(bpy)_2]^{5+}$, **Ru(II)−Os(III)**, obtained by chemical oxidation of the corresponding Ru(II)−Os(II) species, was also briefly investigated.[9] The Ru-based emission was completely quenched on a subnanosecond time scale. This quenching was attributed to photoinduced electron transfer from the excited Ru(II) chromophore to the Os(III) acceptor. No transient intermediates were observed in nanosecond flash photolysis, presumably due to fast charge recombination.

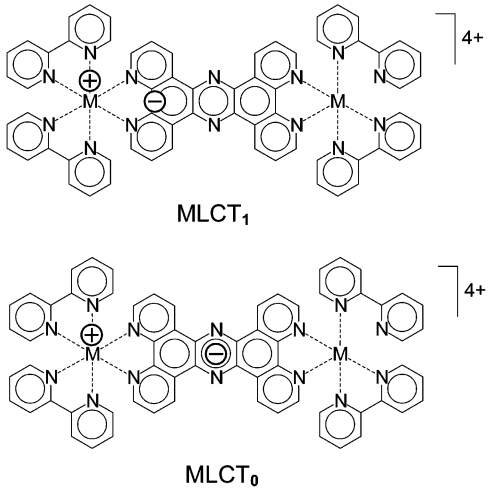

Figure 1. Schematic representation of the two types of metal-to-bridge charge transfer excited states in tpphz binuclear complexes: $MLCT_1$, with main electron density on the bipyridine-like moiety of the bridge; $MLCT_0$, with main electron density on the pyrazine-like moiety of the bridge.

The intramolecular energy transfer and electron transfer quenching observed in **Ru(II)−Os(II)** and **Ru(II)−Os(III)**, respectively, are common processes for Ru−Os polypyridine dyads. The peculiar electronic structure of the tpphz bridging ligand, however, brings further complexity into this standard scheme. Because of the presence of bpy-like and pyrazine-like MLCT states on each chromophore, a variety of stepwise pathways becomes available to energy transfer and electron transfer. In an attempt to unravel these interesting mechanistic possibilities, we have now investigated the **Ru(II)−Os(II)** and **Ru(II)−Os(III)** by ultrafast (femtosecond−picosecond) spectroscopy. A solvent-dependent investigation of the **Ru(II)−Ru(II)** and **Os(II)−Os(II)** homodinuclear species has also been carried out for purposes of comparison.

Experimental Section

Materials. 1,10-Phenanthroline-5,6-dione (phendione),[17] $[Ru(bpy)_2Cl_2]\cdot 2H_2O$,[18] $[Os(bpy)_2Cl_2]\cdot 2H_2O$,[19] $[Ru(bpy)_2(phendione)](PF_6)_2$,[20] $[Ru(bpy)_2(1,10\text{-phenanthroline-5,6-diamine})](PF_6)_2$ ($[Ru(bpy)_2(phendiamine)]$),[21] and $[(bpy)_2Ru(tpphz)Ru(bpy)_2](PF_6)_4$ (tpphz: tetrapyrido-[3,2-*a*:2′,3′-*c*:3″,2″-*h*:2‴,3‴-*j*]phenazine)[22] were prepared according to the literature. $[Os(bpy)_2(phendione)](PF_6)_2$ and $[Os(bpy)_2(phendiamine)](PF_6)_2$ were prepared according to refs 4 and 5 and were purified by chromatography (yields 50 and 45%, respectively). $[(bpy)_2Os(tpphz)Os(bpy)_2](PF_6)_4$ was prepared according to ref 6 and purified by chromatography (yield 82%). $[(bpy)_2Ru(tpphz)Os(bpy)_2](PF_6)_4$ was available from previous work.[9] The mixed valence $[(bpy)_2Ru^{II}(tpphz)Os^{III}(bpy)_2]^{5+}$ species was obtained by oxidation of the $[(bpy)_2Ru(tpphz)Os(bpy)_2]^{4+}$ in CH_3CN/H_2O (10/1 v/v) with stoichiometric

(11) Ishow, E.; Gourdon, A.; Launay, J. P.; Lecante, P.; Verelst, M.; Chiorboli, C.; Scandola, F.; Bignozzi, C. A. *Inorg. Chem.* **1998**, *37*, 3603−3609.
(12) Ishow, E.; Gourdon, A.; Launay, J. P.; Chiorboli, C.; Scandola, F. *Inorg. Chem.* **1999**, *38*, 1504−1510.
(13) Kim, M.-J.; Konduri, R.; Ye, H.; MacDonnell, F. M.; Puntoriero, F.; Serroni, S.; Campagna, S.; Holder, T.; Kinsel, G.; Rajeshwar, K. *Inorg. Chem.* **2002**, *41*, 2471−2476.
(14) A similar situation holds for ruthenium complexes of the related dppz ligand.[15]
(15) Olson, E. J. C.; Hu, D.; Hörmann, A.; Jonkmann, A. M.; Arkin, M. R.; Stemp, E. D. A.; Barton, J. K.; Barbara, P. F. *J. Am. Chem. Soc.* **1997**, *119*, 11458−11467.
(16) Flamigni, L.; Encinas, S.; Berigelletti, F.; MacDonnell, F. M.; Kim, M.-J.; Puntoriero, F.; Campagna, S. *Chem. Commun.* **2000**, 1185−1186.
(17) Yamada, M.; Tanaka, Y.; Yoshimoto, Y.; Kuroda, S.; Shimao, I. *Bull. Chem. Soc. Jpn.* **1992**, *65*, 1006−1010.
(18) Sullivan, B. P.; Salmon, D. J.; Meyer, T. J. *Inorg. Chem.* **1978**, *17*, 3334−3339.
(19) Lay, P. A.; Sargeson, A. M.; Taube, H. *Inorg. Synth.* **1986**, *24*, 291−294.
(20) Goss, C. A.; Abruna, H. D. *Inorg. Chem.* **1985**, *24*, 4263−4267.
(21) Bodige, S.; MacDonnell, F. M. *Tetrahedron Lett.* **1997**, *38*, 8159−8160.
(22) MacDonnell, F. M.; Bodige, S. *Inorg. Chem.* **1996**, *35*, 5758−5759.

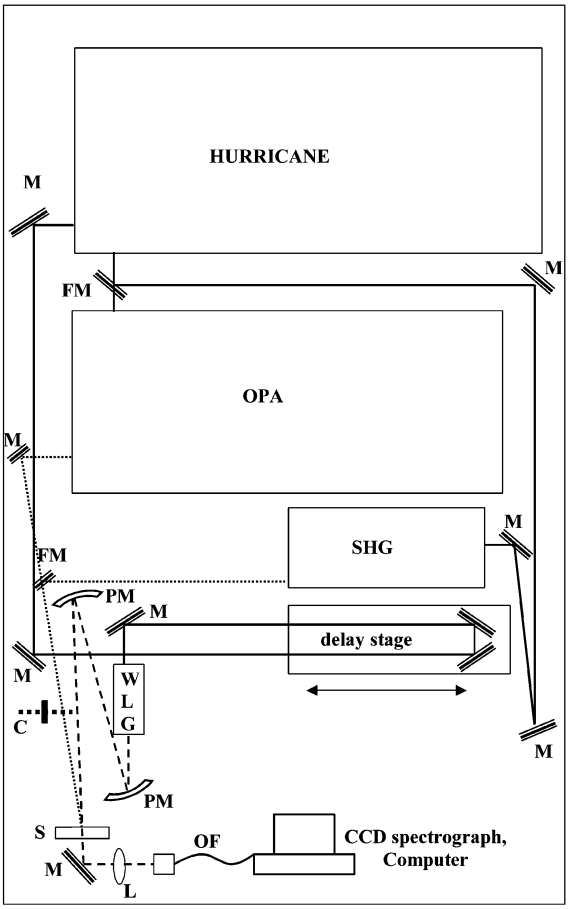

Figure 2. Schematic layout of the ultrafast spectroscopy setup. Continuous line, fundamental (800 nm); dashed line, white light continuum probe; dotted line, pump beam; M, mirror; PM, parabolic mirror; L, lens; OF, optical fiber; S, sample; C, chopper; FM, flipping mirror; OPA, optical parametric amplifier; WLG, white light generator; SHG, second harmonic generator.

amounts of ammonium Ce(IV) nitrate in HNO_3 (6%) solution. Under these conditions, a selective oxidation of the osmium center is obtained.[23]

Apparatus. UV−vis absorption spectra were recorded with a Perkin-Elmer Lambda 40 spectrophotometer. Nanosecond emission lifetimes were measured using a PRA system 3000 time-correlated single photon counting apparatus equipped with a Norland model 5000 MCA card and a hydrogen discharge pulsing lamp (50 kHz, halfwidth 2 ns). The decays were analyzed by means of Edinburgh FLA900 software. To record nanosecond transient absorption spectra and lifetimes, an Applied Photophysics laser flash photolysis apparatus was used, with a Continuum model Surelite II Nd:YAG laser (halfwidth 4−6 ns), frequency doubled (532 nm, 330 mJ) or tripled (355 nm, 160 mJ). The photomultiplier (Hamamatsu R928) signals were processed by means of a LeCroy 9360 (600 MHz, 5 Gs/s) digital oscilloscope.

Ultrafast Transient Absorption Spectroscopy. Femtosecond time-resolved experiments were performed using the spectrometer schematically described in Figure 2. It uses the Spectra-Physics Hurricane system as the laser source. This system comprises a seed laser (Mai Tai, cw diode pumped laser and a mode-locked Ti:sapphire pulsed laser), a pump laser (Evolution, diode-pumped Q-switched Nd:YLF laser), a stretcher, a Ti:sapphire regenerative amplifier, and a compressor. The output of the system consists of pulses of 800 nm, 1 mJ, 100 fs (fwhm) at a repetition rate of 1 kHz.

The design of the pump−probe spectroscopic setup is inspired by the BORODIN spectrometer of Ultrafast Spectrometers, Bowling Green, OH. The Hurricane output is first split (50%) in two beams. One of these (pump) is converted to useful excitation wavelengths by coupling it into a second-harmonic generator (for 400 nm excitation) or into an optical parametric amplifier (Spectra-Physics OPA 800, for tunable wavelengths in the region 320−700 nm). The other (probe) is first passed through a computer-controlled delay line (Physik Instrumente M-415.DG, 150 mm linear positioning stage), and then focused on a 1 mm thick sapphire plate (Crystal System, Inc., HEMLUX grade) to generate a white light continuum (effective useful range, 450−750 nm). The pump beam is passed through a computer controlled optical chopper (Scitec Instruments, 320C) rotating at a frequency of 30 Hz, and focused, with a spot size of about 2 mm, on the sample cell. The sample cell is a 1 mm optical path quartz cylindrical cell (Hellma, 120 QS) placed in a variable-speed rotating holder (courtesy of Prof. L. De Cola, University of Amsterdam). The white light continuum probe beam is collimated and focused into the sample cell, superimposed to the pump beam, at an angle of ca. 5°. To minimize the temporal chirp in the spectrum, parabolic mirrors are used to collimate and focus the white light probe beam. After passing through the sample cell, the white continuum is coupled into a 100 μm optical fiber connected to a CCD spectrograph (Ocean Optics, PC 2000). Typically, time-resolved absorption spectra were acquired averaging over 4000 excitation pulses at any delay time. The delay line, the CCD spectrograph, and the chopper are computer-controlled by a LabVIEW (National Instruments) software routine developed by Ultrafast Spectrometers, Bowling Green, OH. These routines allow automatic spectral acquisition at any selected delay-line settings. Kinetic traces at chosen wavelengths can be extracted from the accumulated transient absorption data.

With 100 fs pump and probe pulses, the effective time resolution of the ultrafast spectrometer, that is, the rise time of an "instantaneous" signal, is ca. 300 fs. The temporal chirp over the 450−750 nm range of the white light probe pulse is ca. 200 fs. The maximum temporal window of the experiment, limited by the optical delay stage, is 0−1000 ps.

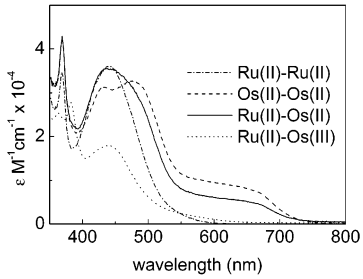

Figure 3. Absorption spectra of the **Ru(II)−Ru(II)**, **Os(II)−Os(II)**, **Ru(II)−Os(II)**, and **Ru(II)−Os(III)** species in CH_3CN.

Results and Discussion

The photophysical behavior of the dinuclear species is known to be solvent sensitive.[9] Therefore, all of the experiments were performed in two solvents of different polarity: CH_2Cl_2 (ϵ = 8.9) and acetonitrile (ϵ = 37.5). The ground-state absorption spectra of the **Ru(II)−Ru(II)**, **Os(II)−Os(II)**, **Ru(II)−Os(II)**, and **Ru(II)−Os(III)** species in CH_3CN are shown in Figure 3. The spectra in CH_2Cl_2 are practically identical. They are dominated by the MLCT transitions of the Ru(II) and Os(II) chromophores. A comparison between the spectra of the different species shows that the Os(II) chromophore differs from the Ru(II) chromophore for (i) a slight red shift in the spin-allowed transitions at 400−550 nm and (ii) a much higher intensity of the spin-forbidden MLCT bands at 550−700 nm. The Os(III) center obviously lacks MLCT transitions and is thus nonchromophoric in this spectral region.

(23) De Cola, L.; Balzani, V.; Barigelletti, F.; Flamigni, L.; Belser, P.; von Zelewsky A.; Frank, M.; Vogtle, F. *Inorg. Chem.* **1993**, *32*, 5228−5238.

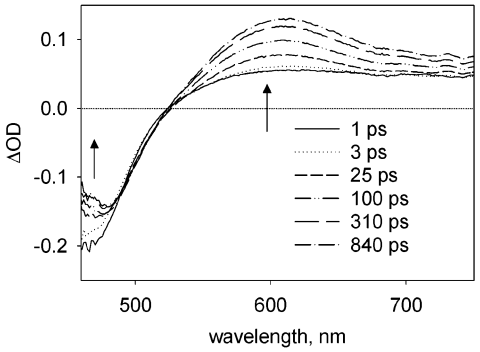

Figure 4. Time-resolved spectral changes observed for **Ru(II)−Ru(II)** in CH_2Cl_2.

The ultrafast spectroscopic experiments were of the pump−probe type, with monochromatic pump and continuous probe (see Experimental Section). The pump wavelength, 400 nm, was convenient for excitation of both the Ru(II) and the Os(II) chromophores. The effective probe spectral window was 450−750 nm. With 100 fs pump and probe pulses, the effective time resolution of the experiments, that is, the rise time of an "instantaneous" signal, is ca. 300 fs. Considering the 200 fs spectral chirp of the probe pulse, the acquisition of meaningful time-resolved spectra is limited to $t > 500$ fs. In the figures with single-wavelength kinetic experiments, the initial 300 fs rise portion of the signal is always omitted for clarity.

The results obtained with the various homo- and heterodinuclear species are summarized and discussed in the following sections.

Ru(II)−Ru(II). From nanosecond experiments, it is known that the long-lived emitting state is of the $MLCT_0$ type (with the excited electron essentially localized in the central pyrazine-like portion of the bridging tpphz).[9] The ultrafast experiments are aimed at time resolving the formation of such a type of state.

In CH_2Cl_2, the initial transient spectrum consists of a strong bleaching of the ground-state absorption (λ_{max} 475 nm) and a broad, positive absorption in the 520−750 nm spectral range (Figure 4). In a very fast process (time constant, ca. 2 ps), there is a partial (ca 10%) recovery of the bleaching, with little change in the positive absorption region. On a longer time scale, the absorbance in the region of the MLCT bleach then remains constant, while a distinct increase in absorption takes place with generation of a pronounced maximum at 610 nm. A single-wavelength (600 nm) kinetic plot is shown in Figure 5a (□), indicating a lifetime for the slow process of 140 ps. The nature of the early (2 ps) process is not known with certainty. It is common to all of the homodinuclear species (see below for Os−Os) and could tentatively be assigned to fast interligand processes converting MLCT states based on the outer bpy ligands to the $MLCT_1$ state based on the tpphz bridge.[24] The slow process (140 ps) with formation of the 610 nm maximum is most probably the same as that observed previously by Flamigni et al.[16,25] and corresponds to intraligand electron transfer (ILET), whereby the $MLCT_1$ state (promoted electron

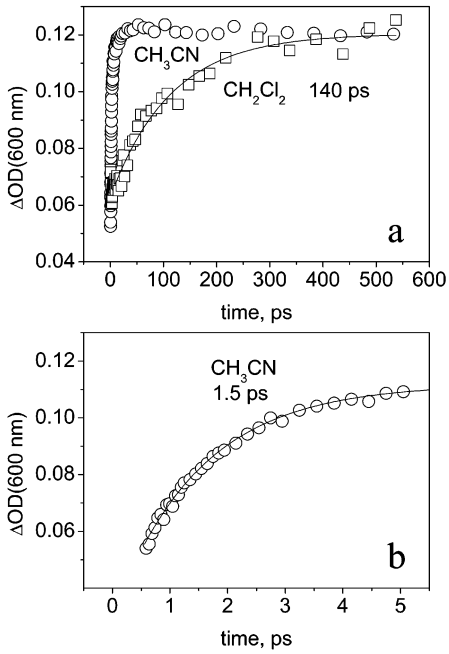

Figure 5. Kinetic plots for **Ru(II)−Ru(II)**. (a) Full time scale, CH_2Cl_2 (□), CH_3CN (○). (b) Expanded view of short time scale in CH_3CN.

mainly localized on the bipyridine-like portion of tpphz) is converted to $MLCT_0$ (promoted electron mainly localized on the pyrazine-like portion of tpphz). In this solvent, the 610 nm $MLCT_0$ absorption reaches a constant value within the time window of the experiment, consistent with the lifetime of 320 ns, as previously measured for the $MLCT_0$ state by nanosecond emission techniques.[9]

In acetonitrile, spectral changes qualitatively similar to those of Figure 4 are observed. However, the increase in absorption with maximum at 610 nm associated with the formation of the $MLCT_0$ state is now much faster (Figure 5a, ○). Analysis of the appropriate kinetic trace (Figure 5b) yields a lifetime of 1.5 ps. Thus, a strong acceleration of the $MLCT_1 \rightarrow MLCT_0$ interconversion is observed when the solvent is changed from dichloromethane to acetonitrile.[26] This can be ascribed to an increased driving force in the more polar solvent, as a consequence of the larger stabilization of $MLCT_0$ (larger charge separation distance) as compared to $MLCT_1$ (smaller charge separation distance). The pronounced bathochromic shift in the emission observed in going from dichloromethane to acetonitrile[9] is consistent with this hypothesis. Once formed, the $MLCT_0$ absorption remains practically constant within the time window of the experiment, consistent with the lifetime of 90 ns, as measured by nanosecond emission techniques.[9]

The photophysical mechanism of **Ru(II)−Ru(II)** in CH_2Cl_2 and CH_3CN is summarized in Figure 6. This simplified[27−29] picture emphasizes the changes in charge distribution taking place along the deactivation path.

(24) Önfelt, B.; Lincoln, P.; Nordén, B.; Baskin, J. S.; Zewail, A. H. *Proc. Natl. Acad. Sci. U.S.A.* **2000**, *97*, 5708−5713.
(25) In ref 16, a lifetime of 230 ps was reported for the same process. Given the strong sensitivity of the kinetics to solvent polarity (vide infra), this discrepancy is probably attributed to a different degree of dryness in the CH_2Cl_2 used.
(26) In acetonitrile, this interconversion could not be observed by Flamigni et al.,[16] due to the time limitation of their apparatus.
(27) In the kinetic schemes, all of the ultrafast processes preceding the formation of $MLCT_1$ (including, e.g., intersystem crossing from the singlet to the triplet manifold[28] and conversion from states based on terminal ligands[24,29]) are collectively indicated by a wavy arrow leading to this state. Approximate energy values of $MLCT_1$ and $MLCT_0$ are estimated from 77 K emission maxima and 298 K emission onset (10%) values, respectively.[9]
(28) Damrauer, N. H.; McCusker, J. K. *J. Phys. Chem. A* **1999**, *103*, 8440−8446.
(29) Shaw, G. B.; Brown, C. L.; Papanikolas, J. N. *J. Phys. Chem. A* **2002**, *106*, 1483−1495.

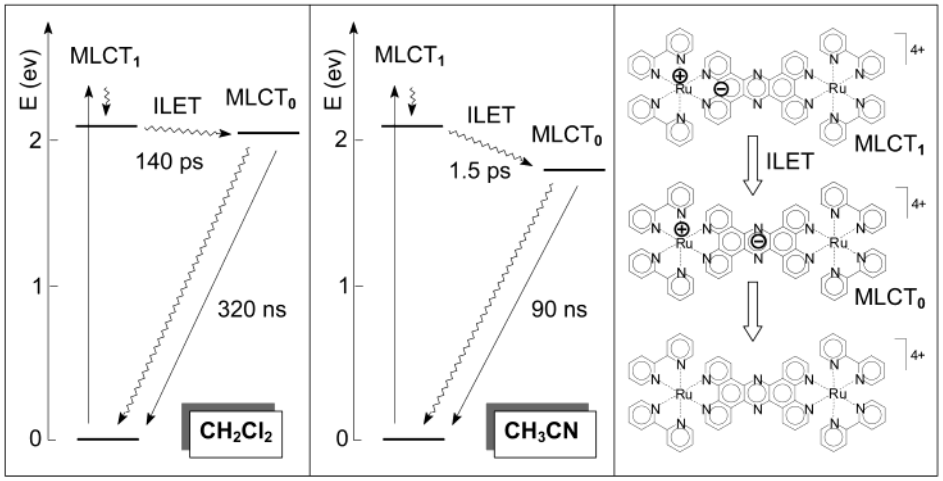

Figure 6. Photophysical mechanism for **Ru(II)−Ru(II)** in CH_2Cl_2 (left) and CH_3CN (center). Schematic picture of the changes in charge distribution along the photophysical pathway (right).

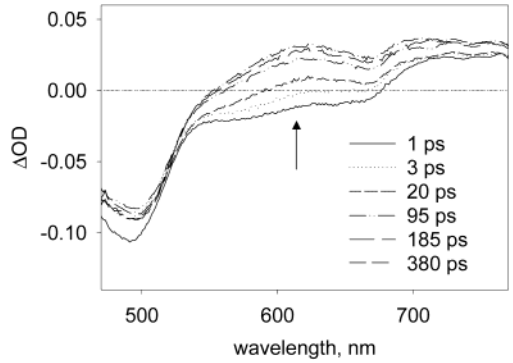

Figure 7. Time-resolved spectral changes observed for **Os(II)−Os(II)** in CH_2Cl_2.

Os(II)−Os(II). From nanosecond experiments, it is known that the long-lived emitting state is of the $MLCT_0$ type (with the excited electron essentially localized in the central pyrazine-like portion of the bridging tpphz).[9] The ultrafast experiments are aimed at time resolving the formation of such a type of state.

In CH_2Cl_2, the initial spectrum consists of a strong bleaching of the ground-state MLCT absorption (λ_{max} 490 nm, extending to 660 nm because of the intense spin-forbidden bands in the osmium system) and a broad, positive absorption in the $\lambda >$ 680 nm range (Figure 7). Here again, after a fast process with partial (ca 10%) recovery of the MLCT bleaching (time constant, ca. 2 ps), a slower increase in absorbance with maximum at 620 nm takes place. Despite the differences in the initial spectrum, the slow spectral changes are remarkably similar in the osmium (Figure 7) and ruthenium (Figure 4) cases, confirming that the slow increase in absorbance with maximum at 620 nm is the spectroscopic signature of ILET interconverting $MLCT_1$ to $MLCT_0$. The lifetime of this process is 130 ps (Figure 8a, □). Within the time window of the experiment, the onset of a slow decay of the $MLCT_0$ absorption is apparent in the osmium case at times longer than 400 ps (Figure 8a, □). This is consistent with the lifetime of $MLCT_0$, 1.5 ns, as measured by nanosecond emission techniques.[9]

In acetonitrile, similar to what happens with the ruthenium dimer, the increase in absorbance with λ_{max} 620 nm is much faster than that in CH_2Cl_2 (Figure 8a, ○). Again, the explanation lies in the larger driving force for the $MLCT_1 \rightarrow MLCT_0$ conversion and is in agreement with the large red shift observed in emission.[9] The time constant of the ILET process is ca. 0.9 ps (Figure 8b). In this solvent, the $MLCT_0$ state decays efficiently to the ground state within the time window of the experiment (Figure 8a, ○). The lifetime, 310 ps, is relatively short, consistent with the expected low energy of this excited state and the energy-gap law. This short lifetime is the reason for the lack of observable emission in acetonitrile solution of the Os−Os dimer.[9]

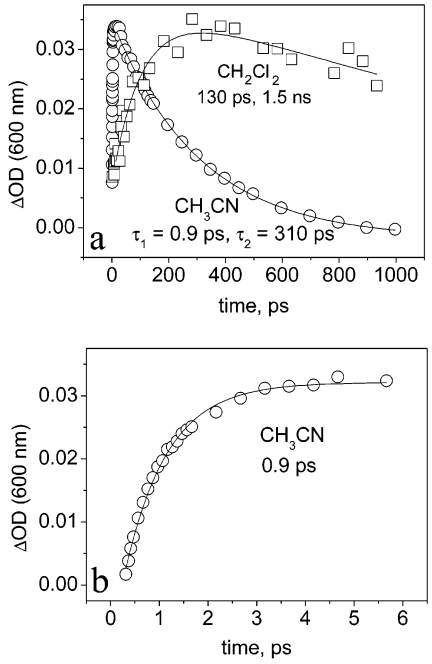

Figure 8. Kinetic plots for **Os(II)−Os(II)**. (a) Full time scale, CH_2Cl_2 (□), CH_3CN (○). (b) Expanded view of short time scale in CH_3CN.

The processes involved in excited-state deactivation of this system are schematized in Figure 9. This simplified[27−29] picture is intended to emphasize the changes in charge distribution along the deactivation path.

Ru(II)−Os(II). The heterobimetallic **Ru(II)−Os(II)** complex is interesting, as the presence of $MLCT_1$ and $MLCT_0$ states on both chromophores provides multiple available pathways for the observed[9] Ru(II) → Os(II) energy transfer process. In Scheme 1, two such possible pathways are indicated: (i) Ru-

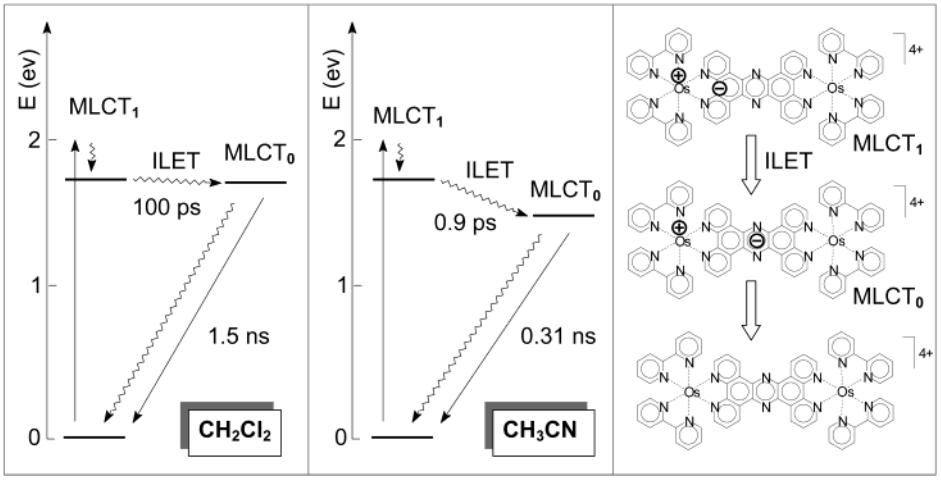

Figure 9. Photophysical mechanism for **Os(II)−Os(II)** in CH_2Cl_2 (left) and CH_3CN (center). Schematic picture of the changes in charge distribution along the photophysical pathway (right).

Scheme 1

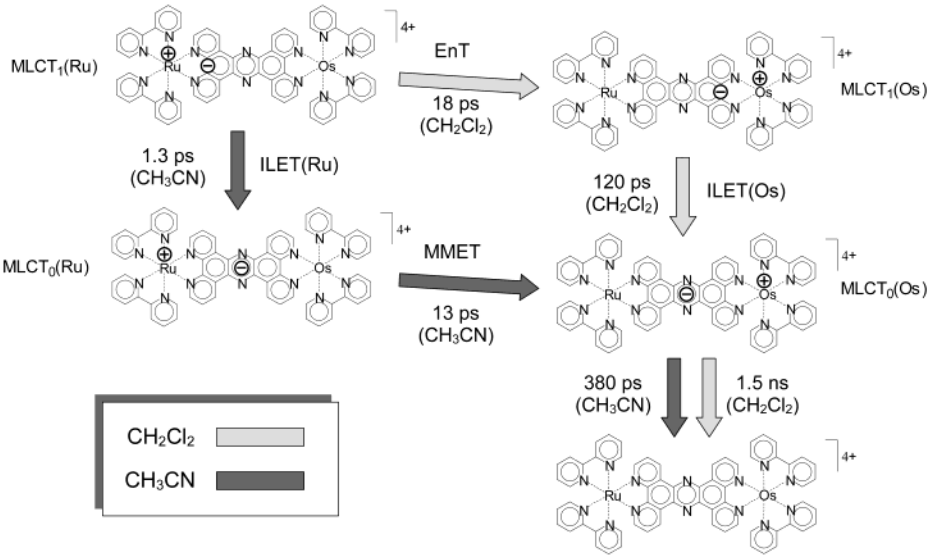

(II) → Os(II) energy transfer at the $MLCT_1$ level (EnT), followed by $MLCT_1$ → $MLCT_0$ relaxation within the Os(II) chromophore (ILET Os); (ii) $MLCT_1$ → $MLCT_0$ relaxation within the Ru(II) chromophore (ILET Ru), followed by Ru(II) → Os(II) energy transfer at the $MLCT_0$ (that, in this schematic representation of the electron distribution, amounts to excited-state metal-to-metal *electron* transfer, MMET).[30] In principle, ultrafast spectroscopy can be used to discriminate between such pathways.

In the heterodinuclear complex, the excitation pulses (400 nm) are absorbed in comparable amounts by both chromophores. Accordingly, the initial spectrum of the Ru−Os species is intermediate between those of the two homobinuclear species (Figure 10). The transient spectroscopy of the heterodinuclear complex in CH_2Cl_2 is characterized by a biphasic behavior (Figure 11). On the time scale of a few tens of picoseconds (Figure 11a), the transient spectrum evolves with a clear red shift in the bleaching region and little change in the absorption region. From kinetic measurements at 490 nm (Figure 11a, inset), the time constant for such a process is 18 ps. On a longer

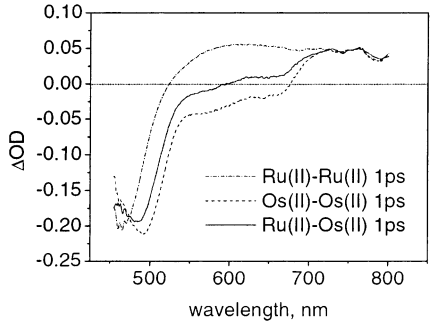

Figure 10. Comparison between the "initial" ($t = 1$ ps) transient spectra of **Ru(II)−Os(II)** (continuous line), **Ru(II)−Ru(II)** (dash−dot line), and **Os(II)−Os(II)** (dashed line) in CH_2Cl_2 solvent.

time scale, an increase in absorption with λ_{max} 620 nm then takes place (Figure 11b). From kinetic measurements at 600 nm (Figure 11b, inset), the time constant for such a process is 190 ps. The first process can be assigned to Ru(II) → Os(II) energy transfer at the $MLCT_1$ level (EnT), on the basis of the characteristic spectral changes (compare Figure 11a with Figure 10). The second process can be confidently assigned to relaxation of the Os-based $MLCT_1$ state to the corresponding $MLCT_0$ state (ILET Os), on the basis of the spectral changes

(30) A third pathway, involving direct conversion from Ru-based $MLCT_1$ to Os-based $MLCT_0$, is considered less likely.

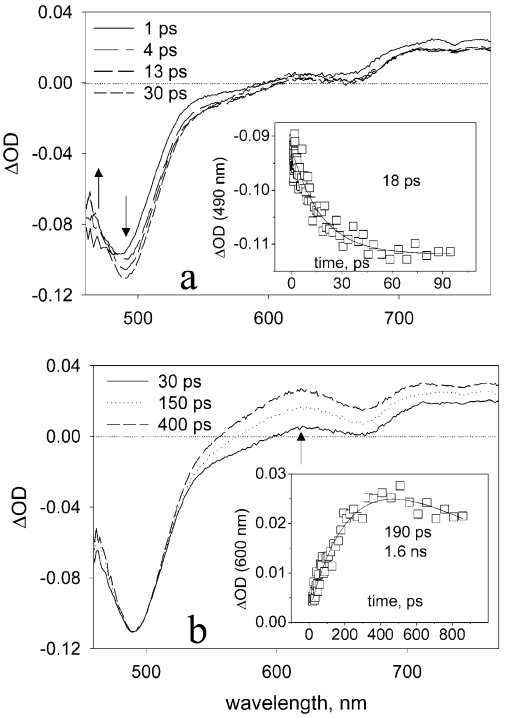

Figure 11. Transient behavior of **Ru(II)−Os(II)** in CH_2Cl_2. (a) Early (t < 30 ps) spectral changes, kinetics at 490 nm (inset). (b) Subsequent (t > 30 ps) spectral changes, kinetics at 600 nm (inset).

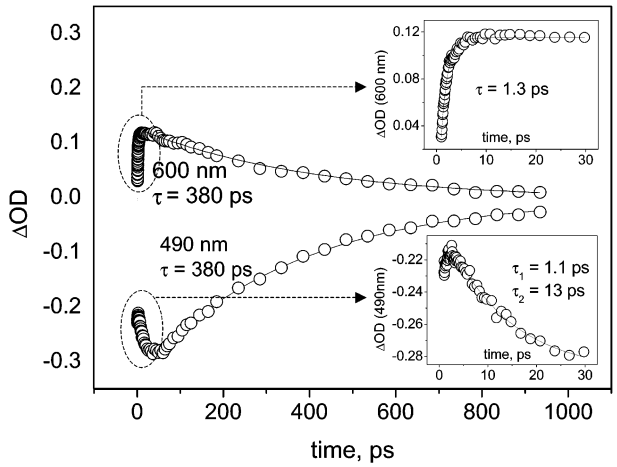

Figure 12. Kinetic plots for **Ru(II)−Os(II)** in CH_3CN at 490 and 600 nm. The insets show expanded views of the two plots in the short (t < 30) time scale.

and the lifetime (that are similar to those observed in Figure 7 for the **Os(II)−Os(II)** system). The final deactivation of the Os-based $MLCT_0$ state in CH_2Cl_2 is known to take place in 1.5 ns,[9] and its onset can be seen within the time window of our experiment (Figure 11b). The observed EnT process is among the fastest reported for Ru(II)−Os(II) polypyridine systems.[31−34] It easily wins the competition with the relaxation of the Ru(II) chromophore (ILET Ru), expected to be slower by an order of magnitude, as inferred from the **Ru(II)−Ru(II)** model. Thus,

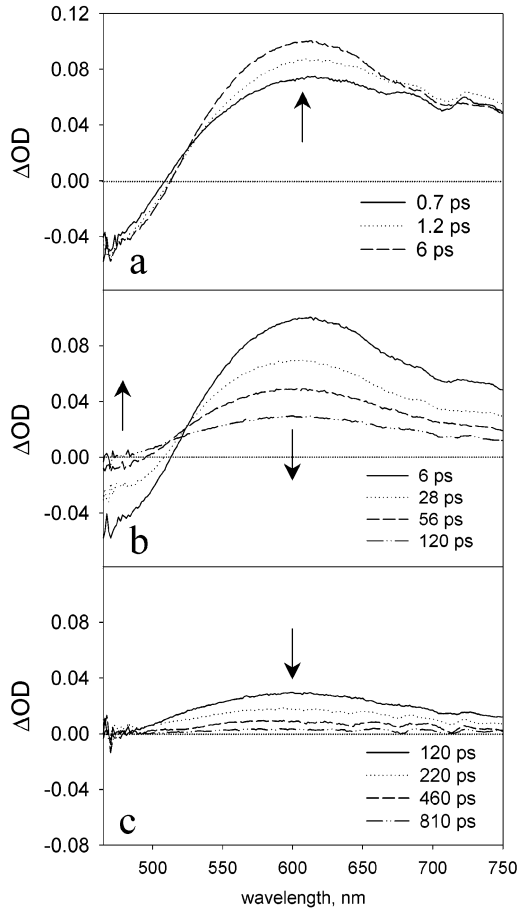

Figure 13. Transient behavior of **Ru(II)−Os(III)** in CH_3CN. (a) Early (t < 6 ps) spectral changes. (b) Spectral changes in the intermediate (6 < t < 120 ps) time regime. (c) Late (t > 120 ps) spectral changes.

in CH_2Cl_2, the pathway EnT + ILET(Os) is followed, as shown in Scheme 1.

The behavior may not necessarily be the same in acetonitrile. In fact, in this solvent, the ILET processes are expected to be strongly accelerated by the larger driving force, as demonstrated by the results on the homodinuclear species. Actually, as shown in Figure 12, the kinetic behavior obtained in acetonitrile is quite different from that observed in CH_2Cl_2. In particular, the increase in absorption at 600 nm, diagnostic of an ILET process, is now the fastest process with a time constant of ca. 1 ps (Figure 12, top inset). The change from the Ru-based to Os-based MLCT state, monitored by the bleaching at 490 nm, is now the subsequent process with a time constant of 13 ps (Figure 12, bottom inset). On a longer time scale, consistent with what happens to the homodinuclear osmium model, the Os-based $MLCT_0$ state decays to the ground state with a time constant of 380 ps (Figure 12). Thus, in acetonitrile, the alternative deactivation pathway is followed: first, relaxation of the Ru-based $MLCT_1$ state to the corresponding $MLCT_0$ state (ILET-(Ru)); then, Ru(II) → Os(II) energy transfer at the $MLCT_0$ level, equivalent to excited-state metal-to-metal electron transfer, MMET). The pathway is shown in Scheme 1.

Ru(II)−Os(III). This species can be obtained from a CH_3-CN solution of the Ru(II)−Os(II) dyad by selective chemical

(31) For instance, an upper limit of 20 ps was reported for *p*-phenylene-bridged systems,[32] and 10−20 ps time constants were measured for alkyne-bridged complexes.[33] Very fast energy transfer processes (200 fs) have been recently observed in Ru(II)−Os(II) dyads bridged by dipyridylpyrazine (dpp).[34]

(32) Sauvage, J.-P.; Collin, J.-P.; Chambron, J.-C.; Guillerez, S.; Coudret, C.; Balzani, V.; Barigelletti, F.; De Cola, L.; Flamigni, L. *Chem. Rev.* **1994**, *94*, 993−1019.

(33) Harriman, A.; Ziessel, R. *Chem. Commun.* **1996**, 1707−1716.

(34) Berglund Baudin, H.; Davidsson, J.; Serroni, S.; Juris, A.; Balzani, V.; Campagna, S.; Hammarström, L. *J. Phys. Chem. A* **2002**, *106*, 4312−4319.

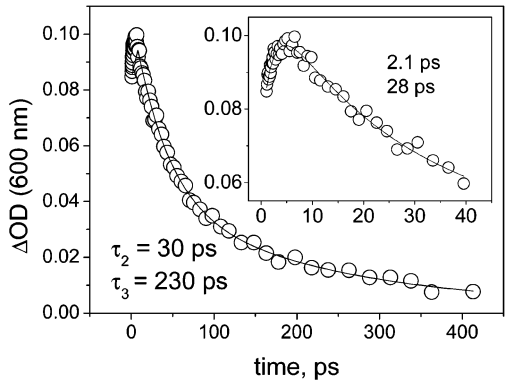

Figure 14. Kinetic plot for **Ru(II)−Os(III)** in CH_3CN at 600 nm. The inset shows an expanded view of the short (t < 40 ps) time scale.

oxidation of the osmium center (E = 0.89 V vs SCE).[9] Upon oxidation, the osmium component loses its chromophoric properties (Figure 3) but becomes a good electron acceptor. In previous work, no appreciable emission from the Ru(II) chromophore was observed, nor any transient absorption could be detected by nanosecond flash photolysis.[9] Therefore, as is common in Ru(II)−Os(III) polypyridine complexes,[4] the efficient quenching was attributed to electron transfer from the excited Ru(II) chromophore to the Os(III) metal center.[9] The quenching process is now investigated by the use of ultrafast spectroscopy. An interesting question pertains to whether the electron transfer quenching takes place directly from the $MLCT_1$ of Ru(II), or rather in a stepwise manner, via ILET. It should be pointed out that, for chemical reasons related to the oxidation reaction, the choice of the solvent was limited in this case to CH_3CN.

The transient spectral changes observed for **Ru(II)−Os(III)** in CH_3CN are shown in Figure 13. The initial spectrum is as expected for a Ru(II) chromophore, with bleaching of the ground state at a short wavelength and absorption by the reduced bridge at a longer wavelength. The transient behavior consists of a sequence of three spectrally distinct steps: (i) a fast increase at 600 nm with little change in the bleaching region (Figure 13a), (ii) a general recovery of both bleaching and transient absorption (Figure 13b), and (iii) a slower decay of residual absorption in the whole spectral region (Figure 13c). The kinetic analysis (Figure 14) shows that the time constants of the three processes are 2.1, 30, and 230 ps. The three processes are assigned as shown in Figure 15. The spectral changes of the first process are typical of ILET and similar in shape and lifetime to those observed for **Ru(II)−Ru(II)** and **Ru(II)−Os(II)** in acetonitrile. The spectral changes observed in the second step are as expected for electron transfer quenching: the 600 nm absorption of the reduced bridging ligand disappears; the formation of the MLCT absorption of the reduced osmium chromophore practically fills up the bleaching of the ruthenium absorption in the 450−500 nm region (where the two chromophores have comparable intensities, see Figure 3) and produces a positive absorption signal at longer wavelengths (where osmium, at difference with ruthenium, has intense spin-forbidden transitions, see Figure 3). This positive absorption is lost in the slower conversion to the ground state by Os → Ru MMET.

In this Ru(II)−Os(III) complex, the quenching of the Ru(II) chromophore is seen to proceed by a sequence of two electron transfer steps (ILET followed by ligand to metal electron transfer). It should be kept in mind that this situation holds in acetonitrile solvent, where ILET is exergonic and very fast. The situation would probably be different (electron transfer occurring directly from $MLCT_1$) in less polar solvents, although such a prediction cannot be practically tested for experimental reasons (see above).

Conclusions

Previous work had shown that aromatic bridges of the tetrapyridophenazine type behave as efficient mediators of energy and electron transfer between metal-based chromophores. Using ultrafast spectroscopy, we have now provided a detailed picture of how this occurs. In fact, because of its complex electronic structure, tpphz plays a more active role than most

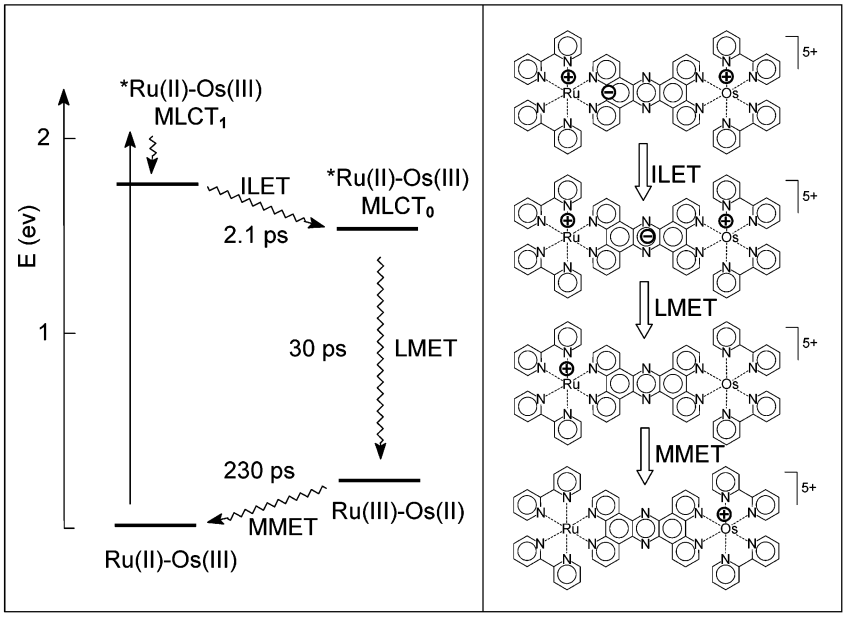

Figure 15. Photophysical mechanism for **Ru(II)−Os(III)** in CH_3CN (left). Schematic picture of the changes in charge distribution along the photophysical pathway (right).

common bridging ligands. The presence of two low-lying π^* orbitals mainly localized on the bpy-like and pyrazine-like portions of the bridge brings about the following distinctive features: (i) $MLCT_1$ and $MLCT_0$ excited states on each chromophore; (ii) multiple solvent-dependent pathways for intramolecular energy transfer; and (iii) a stepwise (electron hopping) pathway for photoinduced electron transfer.

The main results obtained can be summarized as follows:

(1) In homodinuclear complexes, the lowest $MLCT_0$ state is reached from $MLCT_1$ by intraligand electron transfer (ILET). The kinetics is highly sensitive to the solvent, being relatively slow (ca. hundred picoseconds) in CH_2Cl_2 and extremely rapid (few picoseconds) in CH_3CN. This effect is consistent with the greater polarity (and greater stabilization in polar solvents) of $MLCT_0$ relative to $MLCT_1$. The rate constants are very similar for the **Ru(II)−Ru(II)** and **Os(II)−Os(II)** species, as the driving force of ILET is expected to be independent of the metal (Figures 6 and 9).

(2) In the **Ru(II)−Os(II)** heterodinuclear complex, energy transfer from the Ru-based $MLCT_1$ to the Os-based $MLCT_0$ state can occur by two distinct pathways: (a) energy transfer at the $MLCT_1$ level followed by ILET relaxation in the osmium chromophore and (b) ILET relaxation in the ruthenium chromophore followed by Os → Ru metal-to-metal electron transfer. In fact, the first pathway is followed in CH_2Cl_2, whereas the second one takes over in CH_3CN. The switch in mechanism is determined by the solvent sensitivity of the ILET kinetics. Remarkably, for such a complex kinetic scheme, all of the individual steps are time-resolved (Scheme 1).

(3) In the **Ru(II)−Os(III)** mixed-valence species, the photoinduced electron transfer leading from Ru(II)−Os(III) to Ru(III)−Os(II) is, in fact, in CH_3CN, a two-step hopping process: ILET followed by ligand-to-metal electron transfer (Figure 15). On a longer time scale, as usual, charge recombination leads back to the ground state. Although the system is formally a dyad, this behavior actually resembles the stepwise charge separation taking place in molecular triads.[2−4]

Altogether, the results demonstrate that the role of the tpphz bridge is much more than a simple structural one. In fact, the bridging ligand behaves in these systems as a true molecular component, with specific electronic levels that actively participate in the energy and electron transfer processes. As a final comment, the **Ru(II)−Os(II)** case (Scheme 1) provides a striking example of deeply intertwined energy and electron transfer processes. This emphasizes the point[4] that a clear separation between these processes may not be obvious for supramolecular systems characterized by MLCT excited states and electronically active bridging ligands.

Acknowledgment. We are greatly indebted to Alex Gusev and Mihail Zimine for their crucial help in setting up the ultrafast spectrometer. Technical help by Sandro Fracasso is also acknowledged. C.C. and F.S. are grateful to André Gourdon for introducing them to the chemistry of pyridophenazine complexes. Financial support from MIUR (Cofin 1999) is gratefully acknowledged.

JA0284916